Combining Frequency and Spatial Diversities to Calibrate Ranging over WLAN

Jianfeng Yu
School of Computer Science and Technology,
University of Science and Technology of China,
Hefei, 230027, China
justinjf@mail.ustc.edu.cn

Mingjun Xiao
School of Computer Science and Technology,
University of Science and Technology of China,
Hefei, 230027, China
xiaomj@ustc.edu.cn

ABSTRACT

Channel state information (CSI) is now popular in many emerging applications over WLAN, such as gesture recognition, indoor localization, line-of-sight (LOS) identification and ranging. Traditional power-based ranging approaches usually utilize received signal strength indicator (RSSI) because of its low cost and wide applicability. However, the coarse-grained RSSI is sensitive to the multipath effect and performs poorly in the non-line-of-sight (NLOS) situation. Compared with RSSI, CSI is a finer-grained value, and it depicts the amplitude and phase of each frequency-domain subcarrier in an OFDM channel. Besides, MIMO technology leveraged in 802.11 infrastructures extends the spatial diversity of WiFi signals and guarantees reliable communications. To obtain more stable and precise distance of direct path (DDP) between the transmitter and the receiver, we employ both the frequency diversity and spatial diversity of CSI and propose a new ranging system over WLAN. We consider multiple influence factors when implementing the system on commodity WiFi devices, and we evaluate its performance in diverse indoor environments. The results demonstrate that our system outperforms the baselines in all the pre-set scenarios, especially under the conditions of NLOS and dynamic multipaths.

CCS CONCEPTS

• **Human-centered computing → Ubiquitous and mobile computing design and evaluation methods**; • **Computer systems organization → Sensor networks**;

KEYWORDS

Ranging, Channel State Information, WiFi Signal

ACM Reference format:
Jianfeng Yu and Mingjun Xiao. 2017. Combining Frequency and Spatial Diversities to Calibrate Ranging over WLAN. In *Proceedings of the 14th EAI International Conference on Mobile and Ubiquitous Systems: Computing, Networking and Services, Melbourne, VIC, Australia, November 7–10, 2017 (MobiQuitous 2017),* 8 pages.
https://doi.org/10.1145/3144457.3144465

MobiQuitous 2017, November 7–10, 2017, Melbourne, VIC, Australia

ACM ISBN 978-1-4503-5368-7/17/11…$15.00
https://doi.org/10.1145/3144457.3144465

1 INTRODUCTION

Ranging is an essential component of the indoor localizations and aims to get the distance of direct path (DDP) between the transmitter and the receiver. There are a large number of researches exploring the ranging problem [7, 10, 22–24]. Among the various researches, Channel state information (CSI) has been gradually displacing received signal strength indicator (RSSI) as the input of path loss model [9], which is the foundation of the power-based ranging. According to the model, the received signal power decreases monotonically with increasing propagation distance from the transmitter. Thus it is obvious that ranging is accurate only when the propagation distance is equal to DDP or line-of-sight (LOS) distance from the transmitter to the receiver. However, in complicated indoor environment, the LOS signal is always mixed with other non-line-of-sight (NLOS) signals which are from different paths. This phenomenon is termed as multipath effect. The multipath effect usually degrades the propagation model and degenerates the ranging accuracy. RSSI, which depicts an aggregated energy of all the signal paths, is a coarse-grained measurement extracted from the MAC layer and is sensitive to the multipath effect. Besides, the NLOS propagation can decrease the stability of RSSI and exaggerate RSSI fluctuations [4]. Therefore, the distance derived from RSSI is unreliable.

Compared with RSSI, CSI is a finer-grained value reported from the physical (PHY) layer, and it depicts the amplitude and phase of each subcarrier in orthogonal frequency division multiplexing (OFDM) system. Since CSI provides more detailed status information of the wireless communication channels and is more robust to frequency-selective fading, multipath effect and shadowing, it's now popular in many emerging applications over WLAN. In addition to OFDM, there is another key technology, called multiple-input multiple-output (MIMO), leveraged in IEEE 802.11n standard. WiFi devices using MIMO are often equipped with multiple antennas. MIMO extends the spatial diversity of wireless channels to guarantee more reliable communication.

In this work, we propose a new ranging system which combines the frequency and spatial diversities of WiFi signals to calibrate ranging over WLAN. Our system refers to the refined indoor propagation model [22] for calculating the DDP. Theoretically, the length of a propagation path changes one wave length λ, the path will suffer a 2π phase shift, correspondingly [18]. We observe that with rapid environment changes or human motions, CSI values always vary severely because of the phase shifts, which induces ranging results fluctuating apparently. Besides, the imperfection of commercial WiFi devices also lead to notable phase and amplitude offsets of wireless signals. As shown in Fig. 1, there are times when the

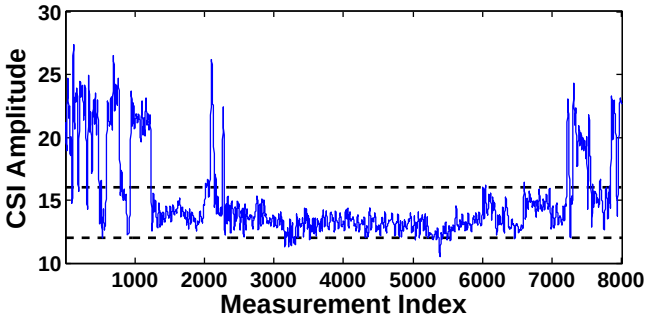

Figure 1: CSI amplitude varies while the receiver is moving

fluctuations are inconspicuous, and we can collect CSI measurements with low and stable variances to alleviate those fluctuations. Then we employ phase calibration, multipath mitigation and traditional signal processing techniques (such as outlier removal and moving average) to eliminate the interference caused by hardware imperfection, multipath effect, sudden impulses and noise. Finally, we combine the frequency and spatial diversities and train the parameters of the model for different transmitter-receiver (TX-RX) antenna pairs to obtain more robust and precise ranging results.

The main contributions of our work are as follows:

(1) We exploit both the frequency and spatial diversities of WiFi signals to calibrate the ranging result over WLAN and propose a new power-based ranging system using the fine-grained CSI.
(2) We utilize phase calibration, multipath mitigation and traditional signal processing techniques to refine the CSI measurements, and employ regression analysis to train the model parameters for different TX-RX antenna pairs and further obtain a synthetic ranging result.
(3) We implement our system in diverse indoor environments and the experimental results demonstrate that our system can significantly improve the ranging accuracy and robustness compared with the baselines.

The rest of the paper is organized as follows. We summarize the related work in Section 2. Section 3 provides some preliminaries. The specific design of our system is introduced in Section 4. Section 5 presents the experiments and evaluates the performance of our system, and Section 6 concludes our work.

2 RELATED WORK

Considering the ubiquitous WiFi devices deployed in indoor environments, *e.g.*, houses, offices, shopping malls and so on, we decide to explore the ranging problem using WiFi signals. Based on the way to calculate the distance using wireless signals, ranging can be divided into two categories: time-based ranging and power-based ranging.

Generally, time-based ranging utilizes the time features of wireless signals, such as time of arrival (TOA) and time difference of arrival (TDOA), to calculate the distance from the transmitter to the receiver. For example, in [3], Gezici et al. introduced the time-based methods for the ultra-wideband (UWB) systems, which have absolute bandwidths of more than 500 MHz. Such wide bandwidths can guarantee either more reliable communications or more accurate ranging results (centimeter accuracy in ranging) compared with WiFi system whose bandwidth is 20 MHz or 40 MHz. Besides, synchronization is an important factor in evaluating the accuracy of UWB positioning systems. Since UWB pulses have very short duration (subnanosecond), clock accuracies and drifts in the target and the reference nodes affect the TOA estimates. Unfortunately, the clocks of a transmitter and a receiver are non-synchronized for WiFi devices, which results in phase error between transceivers. Xie et al. [24] and Vasisht [15] proposed to extend the bandwidth and eliminate the phase error by combing the different frequency bands of WiFi channels, which can help to improve the resolution of TOA. Wen et al. [20] proposed a fine-grained indoor localization system called FILSAM, which also utilizes TOA to calculate the distance. They demonstrated that the AP equipped with more antennas or working on wider bandwidth could help to reduce the ranging error.

Here, we mainly focus on the power-based approaches in which the log-distance path loss model is used to estimate the distance. Conventional methods are usually based on the RSSI values [1, 6, 26]. Although it is convenient to extract RSSI from the MAC layer of WiFi, ZigBee and cellular networks, RSSI is sensitive to multipath effect and fluctuates dramatically in complicated indoor environment. We tend to exploit the new metric, namely channel state information (CSI), which surpasses RSSI in ranging, and there have been various researches exploring the availability of CSI in the areas of mobile and ubiquitous computing, such as motion or gesture recognition [12, 16–18], LOS identification [21], indoor localization [10, 11, 22, 23] and entertainment [8]. In order to realize meter-level ranging, Sen et al. [11] proposed a spot localization system, called PinLoc, and it exploits CSI distributions (fingerprints) of every 1 $m \times 1$ m spot in time and frequency domain to distinguish different positions by a pattern-matching process. The FIFS system proposed by Xiao et al. [23] uses the weighted average CSI values over multiple antennas as the fingerprints to realize ranging or positioning. Moreover, Wang et al. [19] developed DeepFi, which generates feature-based fingerprints by utilizing a larger number of weights obtained by deep learning for different locations. Nevertheless, it usually costs lots of computational resources and labor force when building and updating the fingerprint database [7].

In order to establish the relationship between the CSI measurement and distance, Wu et al. [22] proposed a refined indoor propagation model termed as FILA, and they tried to remove components representing multipath reflections in the power delay profile and retain the first component including the LOS path to mitigate the influence of propagation paths with long delay as that in [10]. However, they only considered the multipath effect when ranging but ignored the influences of hardware imperfection and spatial diversity of WiFi signals. In this work, multiple influence factors, such as hardware imperfection, multipath effect, dynamic multipath (movement of transmitter/receiver and/or reflectors), are taken into consideration when refine the CSI measurements, and we exploit both the frequency and spatial diversities of WiFi signals to propose a more robust and precise ranging system compared with FILA [22] and a RSSI-based system.

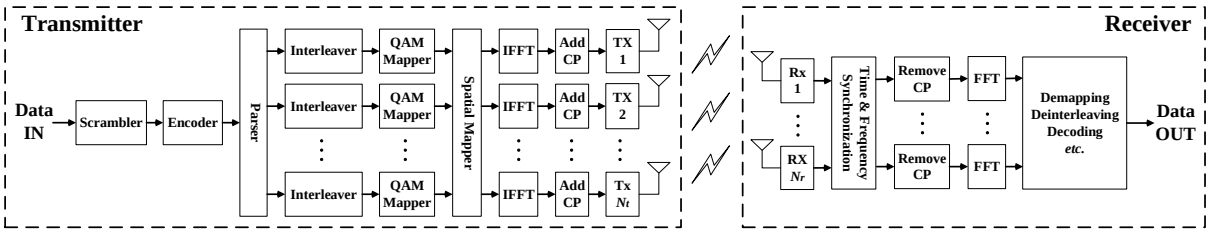

Figure 2: The framework of MIMO OFDM system. The transmitter has N_t antennas and the receiver has N_r antennas.

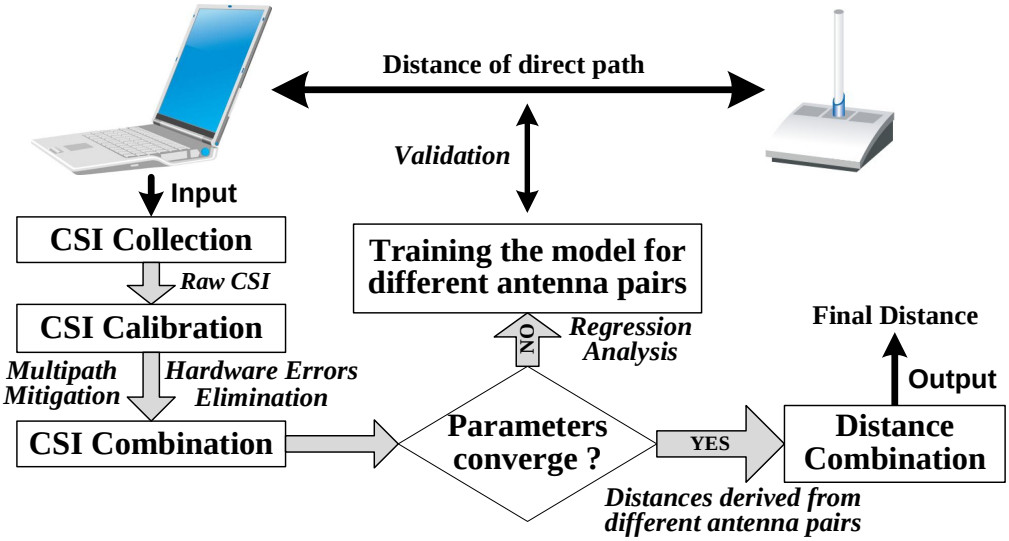

Figure 3: The architecture of our system

3 PRELIMINARIES

3.1 OFDM & MIMO

In IEEE 802.11n wireless LAN standard, OFDM and MIMO are two key physical layer (PHY) technologies [14], and they are combined to be the MIMO OFDM system. On the transmitter side, OFDM divides a high-rate data stream into many parallel low-rate data streams and distributes them across multiple closely spaced, orthogonal subcarriers. Then the frequency-domain subcarriers are converted into time-domain OFDM symbols via inverse fast fourier transform (IFFT). Finally, every symbol is added with a cyclic prefix (CP) to prevent inter-symbol interference (ISI) before transmitted into the air through multiple TX antennas. While receiving signals, the receiver executes nearly opposite operations to obtain the original data. More specifically, the fast fourier transform (FFT) procedure can convert the received signals back to the frequency domain. Thus, OFDM turns the frequency-selective channel into a set of parallel flat fading subcarriers and dramatically improves the efficiency of bandwidth.

As for MIMO, it enhances the capacity of the radio link by transmitting multiple signals over multiple co-located antennas at one or both sides without additional power or bandwidth expenditure [2]. Space-time coding [13] is employed to guarantee that the signals transmitted over different antennas are orthogonal to each other, and it will be easier for the receiver to separate all the signals. Fig. 2 depicts the framework of MIMO OFDM system, and there are N_t TX antennas and N_r RX antennas. Our system utilizes both the frequency diversity and spatial diversity to reduce the ranging error.

3.2 Channel State Information

In the frequency domain, channel frequency response (CFR) characterizes the small-scale multipath effect and the frequency-selective fading caused by the constructive and destructive phases [25]. In MIMO OFDM system, the complex valued CFR can be expressed as

$$H(f_s) = \sum_{k=1}^{N} \alpha_k e^{-j2\pi f_s \tau_k}, \tag{1}$$

where f_s is the frequency of subcarrier s, and N, α_k and τ_k represent the total number of multipaths, the amplitude and the propagation delay of a specific path k, respectively. CSI is a sample version of CFR and it is employed in the commodity WiFi network interface cards (NICs) to monitor the channel properties. CSI depicts fine-grained signal strength and phase information of OFDM subcarriers between every pair of TX-RX antennas from one OFDM frame. With the tool in [5], we can obtain a CSI measurement containing 30 matrices with dimensions $N_t \times N_r$ from one OFDM frame and

these 30 matrices represent the discrete CFR of 30 selected OFDM subcarriers. Thus, our system can simultaneously use $30 \times N_t \times N_r$ values to calculate the distance from one measurement.

3.3 Channel Impulse Response

In theory, the wireless propagation channel is modeled as a temporal linear filter, known as channel impulse response (CIR) [9]. Since CFR is the Fourier transform of CIR, and CIR can be derived from Eq. (1) by IFFT. Thus the CIR h at time t is denoted as

$$h(t) = \sum_{k=1}^{N} \alpha_k \delta(t - \tau_k), \tag{2}$$

where $\delta(\cdot)$ is the Dirac delta function and the residual parameters have the same meanings as they are in Eq. (1), and every impulse represents a multipath component.

4 DESIGN

The proposed method utilizes fine-grained CSI to realize a more robust and precise ranging system compared with traditional RSSI-based approach in the indoor environment. The architecture of our system is shown in Fig. 3 and the detailed design is as follows.

4.1 CSI Collection

IEEE 802.11n operates on both the 2.4 GHz and the lesser-used 5 GHz bands. Since the 2.4 GHz band is narrower and more crowded than the 5 GHz band, the latter is a much better choice for ensuring the top speed and stable communications. Therefore, we run the system on the 5 GHz band and employ a fixed-size receive window to collect the CSI measurements. We process the full samples in the window every time, if the variance of the received samples exceeds the threshold $\sigma^2_{threshold}$, we then discard the unsatisfactory data and restart the collection procedure. Otherwise, we store the samples, which fluctuate between the dotted lines in Fig. 1, and continue the following processes. Because the sample rate is high enough, *e.g.*, 2 KHz, it will take little time to obtain the relatively stable CSI measurements even if the transmitter/receiver and/or the reflectors are moving (named dynamic multipaths).

4.2 CSI Calibration

The satisfactory CSI measurements contain the signal distortions due to channel propagation (*e.g.*, path loss, multipath effect and shadowing) and hardware imperfection (*e.g.*, power control uncertainty, central frequency offset (CFO) and packet boundary detection (PBD) error [24]). It is necessary to calibrate the raw CSI measurements and obtain effective values.

4.2.1 ***Hardware Error Elimination.*** Hardware imperfection is a non-trivial interference factor leading to the change of amplitudes and phases of received signals, which blurs the characteristics of channel propagation. Before multipath mitigation, we need to eliminate the measurement errors induced by the WiFi devices. Power control uncertainty mainly influences the CSI amplitude and can be compensated by averaging. CFO and PBD result in phase error, and the measured phase of the s^{th} ($s = 1, 2, ..., S$) subcarrier in S subcarriers of one TX-RX antenna pair can be simply denoted as $\widetilde{\phi_s} = \phi_s + s \cdot \phi_{PBD} + \beta + Z$, where ϕ_s is the phase offset caused by channel propagation, ϕ_{PBD} is the phase error induced by PBD and multiplied with subcarrier index s, β is the phase error induced by CFO, Z is the small measurement noise which can be omitted. According to [24], β has no impact on the derived CIR, and $\phi_{PBD} \sim N(0, \sigma^2)$, thus ϕ_{PBD} can be removed by averaging over multiple measured CSI phases in terms of the weak law of large numbers:

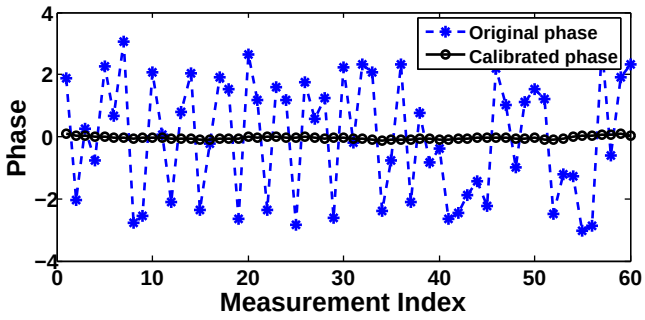

Figure 4: Original phases vs calibrated phases of CSI measurements

$$\overline{\phi}_s = \frac{1}{m} \sum_{k=1}^{m} \widetilde{\phi}_s(k), \tag{3}$$

where $\widetilde{\phi}_s(k)$ stands for the k^{th} CSI phase value of the subcarrier s, m is the CSI amount. Fig. 4 illustrates the result of the calibrated phases, and they distribute relatively stably.

4.2.2 ***Multipath Mitigation.*** Multipath mitigation is the major concern of our design, and it is challenging. Theoretically, we can separate every propagation path from CIR in terms of Eq. (2), but the bandwidth of a 802.11n wireless channel is 20 MHz, and the resolution of CIR is approximately 1/20MHz = 50 ns, as shown in Fig. 5(a), we can't distinguish every signal path from the low-resolution CIR but total $S(= 30)$ path clusters. Moreover, the direct path traverses the minimum distance and its time delay likely appears in the earliest component of the CIR. The first several components generally contain the direct propagation path and other reflected NLOS paths whose travel time is similar to the direct path. Therefore, we can retain the first M ($1 \le M \le S$) components and wipe out the residual components of CIR to alleviate the multipath effect. Fig. 5(b) illustrates the change of CSI amplitudes when the last 15 multipath components of a measurement are sanitized, and this apparently reduces the fading degrees cross the overall subcarriers. Besides, our system can dynamically adjust M in order to obtain the optimal ranging accuracy while training the parameters of the propagation model.

4.3 CSI Combination

Since the channel bandwidth of 802.11n is larger than the coherence bandwidth, all the 30 subcarriers of each TX-RX antenna pair fade independently and the fadings are frequency-selective. By leveraging the frequency diversity of CSI, it is feasible to alleviate the fadings occurring on every single subcarrier. We calculate weighted average of all subcarriers for obtaining a robust combination C against the

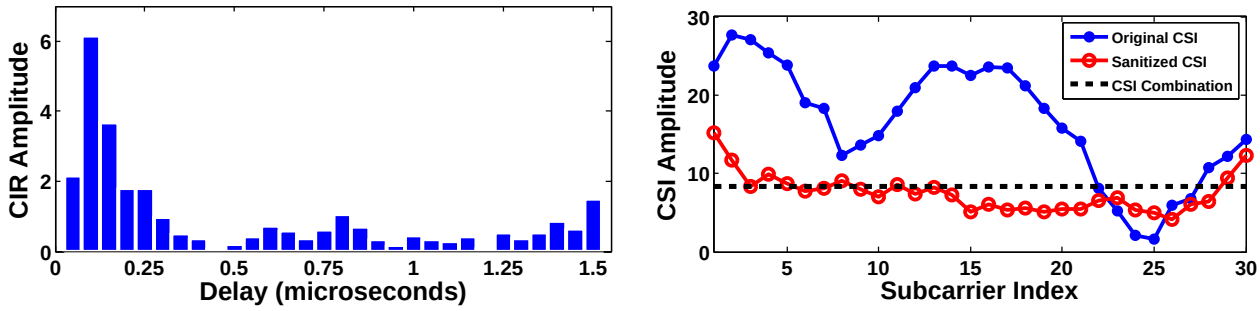

(a) (b)

Figure 5: (a) CIR of one measurement. (b) Comparison of the per-subcarrier amplitude of the measurement shown in (a) before and after sanitizing the last 15 multipath components, and the dotted line represents the combination of sanitized CSI subcarriers.

frequency-selective fading, and the subcarriers are allocated with diverse weights which are relative to their frequency. Thus, the CSI combination of the antenna pair (i, j) $(1 \le i \le N_t, 1 \le j \le N_r)$ is expressed as

$$C(i,j) = \frac{1}{S}\sum_{s=1}^{S}\frac{f_{k_s}}{f_0}\mathrm{A}_s(i,j), \tag{4}$$

where k_s ($k_s \in$ {-28, -26, -24, -22, -20, -18, -16, -14, -12, -10, -8, -6, -4, -2, -1, 1, 3, 5, 7, 9, 11, 13, 15, 17, 19, 21, 23, 25, 27, 28}) is the subcarrier index of one OFDM channel in practice, f_0 is the central frequency, A_s is the amplitude of subcarrier s. The dotted line in Fig. 5(b) represents the combination of the sanitized CSI values.

In addition, outlier removal and moving average are employed to eliminate the sudden impulses and noise of the combinations.

4.4 Distance Computation

We refer to the refined indoor propagation model proposed in [22] to establish the relationship between the CSI combination and distance, and the model is expressed as

$$d = \frac{1}{4\pi}\left[\left(\frac{c}{f_0 \times C}\right)^2 \times \xi\right]^{\frac{1}{n}}, \tag{5}$$

where c is the wave velocity (equals 3×10^8 m/s), ξ is the environment factor and n is the path loss exponent. ξ and n are environment-related, and need to be trained in different environments. Eq. (5) can be rewritten as

$$\log(4\pi d) = -\frac{2}{n}\log C + \frac{1}{n}\log\left(\frac{c^2 \times \xi}{f_0^2}\right). \tag{6}$$

Eq. (6) is similar to the pattern $Y = p1 \cdot X + p0$, thus we can employ regression analysis to train the parameters of every TX-RX antenna pair and further obtain the specific models of a particular environment. Considering the spatial diversity, the final DDP, named distance combination, can be denoted as the sum of the weighted distances derived from multiple antenna pairs:

$$\overline{d} = \sum_{\substack{1 \le i \le N_t \\ 1 \le j \le N_r}} \omega_d(i,j)d(i,j), \tag{7}$$

where $d(i, j)$ is the DDP derived from the antenna pair (i, j), $\omega_d(i, j)$ is the weight which is inversely proportional to the ranging error of the antenna pair (i, j), and $\sum \omega_d(i, j) = 1$. Our system can easily be extended to the indoor localization application when multiple access points (APs) are applied or the angle-of-arrival (AoA) is known. Since training the model is a simple linear regression problem, it will not take lots of time to compute the parameters.

5 EXPERIMENT & EVALUATION

5.1 Experimental Setup

5.1.1 ***Hardware Setup.*** We use a TP-LINK TL-WDR4300 wireless router as the transmitter, and a 3.3GHz Intel(R) Core i5 CPU 4GB RAM desktop computer equipped with an Intel 5300 NIC as the receiver. The transmitter is installed with 2 omni-directional antennas and operates in IEEE 802.11n AP mode at 5.745GHz (channel 149). The receiver has 3 omni-directional antennas and its firmware is modified using the tool in [5] so as to report the CSI measurements one of which contains 2×3 CSI streams. On the transmitter side, we utilize *pktgen* module of Ubuntu 12.04 operation system to continuously send packets to the receiver. Meanwhile, the rate of receiving packets can nearly reach 1000 packets per second on the receiver side, and the size of receive window is empirically set as 50.

5.1.2 ***Experimental Scenarios.*** We conduct the experiments in three different scenarios in our institute, as is shown in Fig. 6:

- *Meeting Room*: The size of the meeting room is $5\ m \times 8\ m$ and there is merely a little office furniture. Both transmitter and receiver are put on the council board, and the transmitter is fixed while the receiver is moved to different positions with different distances from the transmitter. Since there is no obstacle between the TX antennas and RX antennas and the reflectors are static, which can be regarded as a relatively ideal indoor environment.
- *Corridor*: The corridor is outside our laboratory and its size is $3\ m \times 12\ m$. We deploy the transmitter inside and outside of the laboratory respectively to explore the impact of absence of LOS while ranging.

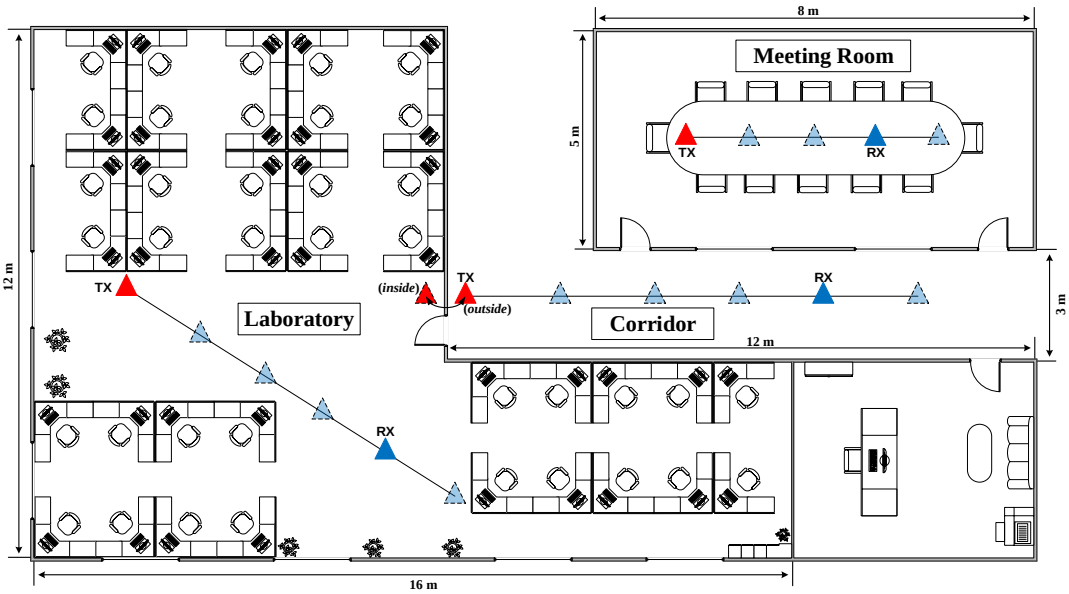

Figure 6: Experimental scenarios

- *Laboratory*: The maximum length and width of our laboratory are 16 *m* and 12 *m* respectively, and there are approximately 40 seats. We put the transmitter at the place which is marked as a red triangle, and move the receiver to the pre-set points along the path (a solid line in Fig. 6). There are students typing or walking when we are ranging. This experiment is conducted to evaluate the robustness of our system.

In each scenario, we collect both the CSI and RSSI at the same time and implement the FILA system proposed in [22] and a RSSI-based ranging system as the baselines to make a comparison with our system. The evaluation results are described as follows.

5.2 Performance Evaluation

5.2.1 ***Overall Performance.*** We use cumulative distribution function (CDF) of ranging errors to quantify the performance of all the systems. Fig. 7(a) - 7(c) illustrate the ranging errors of different systems in different scenarios, and our system outperforms the baselines in all these environments. In the meeting room, the maximal ranging error of our system is less than 1.2 *m* which is nearly one fourth of the error of the RSSI-based system, and the performance of FILA is close to but a little poorer than ours. Besides, almost half of the errors of our system are less than 0.5 *m*.

Compared with the meeting room, there are more reflectors in the corridor scenario, such as stairs, iron railings, which increase the multipaths and lead to the maximal error of 2 *m* for our system, 5.5 *m* for the RSSI-based system and 2.55 *m* for FILA, respectively.

Moreover, the environment of laboratory is much more complicated for containing more static multipaths and many dynamic multipaths caused by people moving and typing. However, the 80% error of our system can still be around 1.8 *m* while the error of the RSSI-based system is larger than 4 *m* and the error of FILA is around 3 *m*. The accuracy of our system is 5-6 times better than that of the RSSI-based system at the point of 100%.

These results demonstrate that the proposed system is more robust in diverse environments and provides more precise ranging compared with the RSSI-based system and FILA system.

5.2.2 ***Impact of LOS.*** As shown in Fig. 8(a), when we hide the transmitter inside the laboratory and block the LOS path towards the receiver, it has great influence on the RSSI-based system, and its accuracy drops significantly. However, our system can still achieve high ranging accuracy (approximately, 1.9 *m*) which is also larger than FILA (approximately, 2.7 *m*). Fig. 8(b) depicts the difference of ranging error of our system under the condition of LOS and NLOS, which also demonstrates that our system is robust for the changes of surroundings.

5.2.3 ***Impact of Multipath.*** Multipath effect can be alleviated by removing the long-delay components of CIR, and Fig. 9 illustrates the ranging errors with different numbers of reserved components. With the removal of multipath components, the accuracy is improved as expected. However, the accuracy does not increase with reduction of components all the time, and our system performs better with 10 reserved multipath components than that with 2 components. We observe that the best ranging accuracy of our system often happens when the first 8–12 components are reserved.

5.2.4 ***Impact of Spatial Diversity.*** In the experiment, we explore the spatial diversity of WiFi signals and utilize the weighted average of distances derived from multiple TX-RX antenna pairs to improve the final ranging accuracy. Although the distance errors introduced from different antenna pairs may be constructive or destructive, we observe that our system does achieve more robust and precise ranging by combining all the 6 TX-RX antenna pairs, as is shown in Fig. 10.

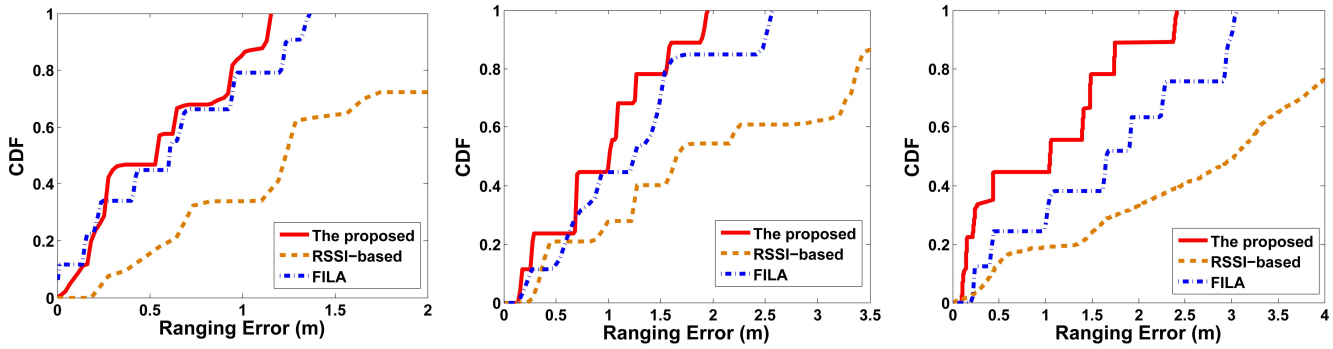

(a) Meeting Room (b) Corridor (c) Laboratory

Figure 7: The comparison of ranging errors of different systems in different scenarios

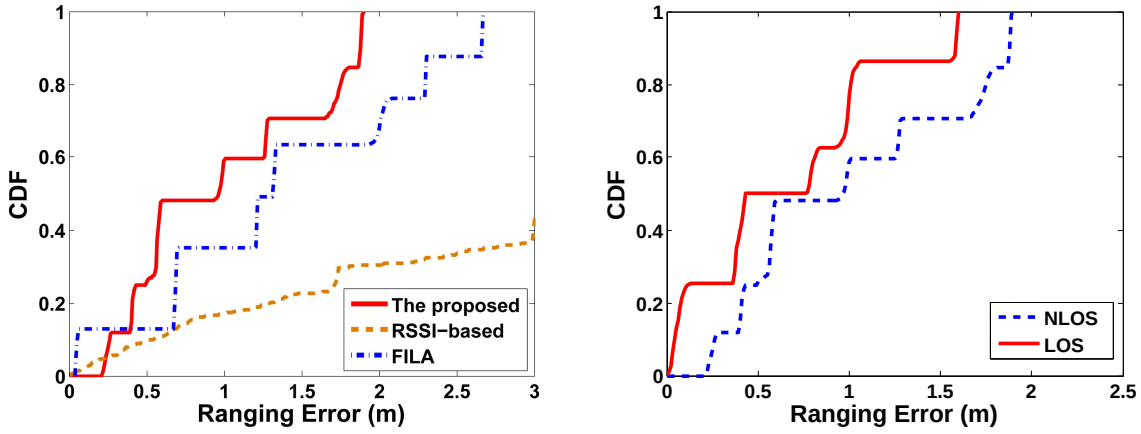

(a) (b)

Figure 8: (a) The comparison of ranging error without LOS. (b) The impacts of LOS and NLOS on our system

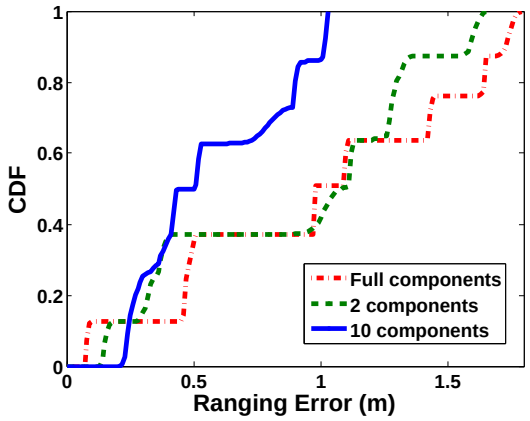

Figure 9: The comparison of ranging error with different number of reserved multipath components

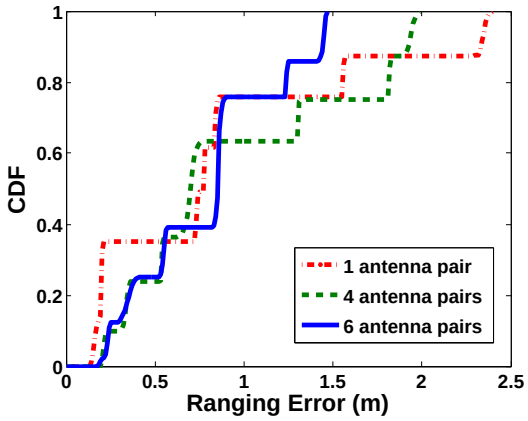

Figure 10: The comparison of ranging error with different TX-RX antenna pairs

6 CONCLUSIONS

In this work, we have exploited the frequency and spatial diversities of CSI extracted from the PHY layer of WLAN, and proposed a new ranging system using both the OFDM and MIMO technologies. We have implemented our system in several different indoor scenarios, and compared it with two different baselines. The experimental results demonstrate that our system outperforms the baselines in all the pre-set environments, especially under the conditions of NLOS and dynamic multipaths. The proposed system is expected to be more robust and precise in ranging. We will carry on the deep study of ranging over WLAN, and try to apply it in the indoor localization applications or extend it to the next-generation mobile networks in the future work.

ACKNOWLEDGEMENTS

This work was supported in part by the National Natural Science Foundation of China(NSFC) (Grant No.61572457, 61379132, U1301256, 61502261, 61303206, 61572342) and the Natural Science Foundation of Jiangsu Province in China (Grant No.BK20131174, BK2009150).

REFERENCES

[1] Paramvir Bahl and Venkata N Padmanabhan. 2000. RADAR: An in-building RF-based user location and tracking system. In *INFOCOM 2000. Nineteenth Annual Joint Conference of the IEEE Computer and Communications Societies. Proceedings. IEEE*, Vol. 2. Ieee, 775–784.

[2] Helmut Bölcskei. 2006. MIMO-OFDM wireless systems: basics, perspectives, and challenges. *Wireless Communications, IEEE* 13, 4 (2006), 31–37.

[3] Sinan Gezici, Zhi Tian, Georgios B Giannakis, Hisashi Kobayashi, Andreas F Molisch, H Vincent Poor, and Zafer Sahinoglu. 2005. Localization via ultra-wideband radios: a look at positioning aspects for future sensor networks. *Signal Processing Magazine, IEEE* 22, 4 (2005), 70–84.

[4] Daniel Halperin, Wenjun Hu, Anmol Sheth, and David Wetherall. 2011. Predictable 802.11 packet delivery from wireless channel measurements. *ACM SIGCOMM Computer Communication Review* 41, 4 (2011), 159–170.

[5] Daniel Halperin, Wenjun Hu, Anmol Sheth, and David Wetherall. 2011. Tool release: gathering 802.11 n traces with channel state information. *ACM SIGCOMM Computer Communication Review* 41, 1 (2011), 53–53.

[6] Juan Liu, Ying Zhang, and Feng Zhao. 2006. Robust distributed node localization with error management. In *Proceedings of the 7th ACM international symposium on Mobile ad hoc networking and computing*. ACM, 250–261.

[7] Alex T Mariakakis, Souvik Sen, Jeongkeun Lee, and Kyu-Han Kim. 2014. Sail: Single access point-based indoor localization. In *Proceedings of the 12th annual international conference on Mobile systems, applications, and services*. ACM, 315–328.

[8] Kun Qian, Chenshu Wu, Zimu Zhou, Yue Zheng, Zheng Yang, and Yunhao Liu. 2017. Inferring Motion Direction using Commodity Wi-Fi for Interactive Exergames. In *Proceedings of the 2017 CHI Conference on Human Factors in Computing Systems*. ACM, 1961–1972.

[9] Theodore S Rappaport et al. 1996. *Wireless communications: principles and practice*. Vol. 2. Prentice Hall PTR New Jersey.

[10] Souvik Sen, Jeongkeun Lee, Kyu-Han Kim, and Paul Congdon. 2013. Avoiding multipath to revive inbuilding WiFi localization. In *Proceeding of the 11th annual international conference on Mobile systems, applications, and services*. ACM, 249–262.

[11] Souvik Sen, Božidar Radunovic, Romit Roy Choudhury, and Tom Minka. 2012. You are facing the Mona Lisa: spot localization using PHY layer information. In *Proceedings of the 10th international conference on Mobile systems, applications, and services*. ACM, 183–196.

[12] Sheng Tan and Jie Yang. 2016. WiFinger: leveraging commodity WiFi for fine-grained finger gesture recognition. In *Proceedings of the 17th ACM International Symposium on Mobile Ad Hoc Networking and Computing*. ACM, 201–210.

[13] Vahid Tarokh, Nambi Seshadri, and A Robert Calderbank. 1998. Space-time codes for high data rate wireless communication: Performance criterion and code construction. *Information Theory, IEEE Transactions on* 44, 2 (1998), 744–765.

[14] Richard Van Nee, VK Jones, Geert Awater, Allert Van Zelst, James Gardner, and Greg Steele. 2006. The 802.11 n MIMO-OFDM standard for wireless LAN and beyond. *Wireless Personal Communications* 37, 3-4 (2006), 445–453.

[15] Deepak Vasisht, Swarun Kumar, and Dina Katabi. 2016. Decimeter-Level Localization with a Single WiFi Access Point.. In *NSDI*. 165–178.

[16] Guanhua Wang, Yongpan Zou, Zimu Zhou, Kaishun Wu, and Lionel M Ni. 2014. We can hear you with wi-fi!. In *Proceedings of the 20th annual international conference on Mobile computing and networking*. ACM, 593–604.

[17] Hao Wang, Daqing Zhang, Yasha Wang, Junyi Ma, Yuxiang Wang, and Shengjie Li. 2016. RT-Fall: A Real-time and Contactless Fall Detection System with Commodity WiFi Devices. *IEEE Transactions on Mobile Computing* (2016).

[18] Wei Wang, Alex X Liu, Muhammad Shahzad, Kang Ling, and Sanglu Lu. 2015. Understanding and modeling of wifi signal based human activity recognition. In *Proceedings of the 21st Annual International Conference on Mobile Computing and Networking*. ACM, 65–76.

[19] Xuyu Wang, Lingjun Gao, Shiwen Mao, and Santosh Pandey. 2017. CSI-based fingerprinting for indoor localization: A deep learning approach. *IEEE Transactions on Vehicular Technology* 66, 1 (2017), 763–776.

[20] Fuxi Wen and Chen Liang. 2015. Fine-grained indoor localization using single access point with multiple antennas. *IEEE Sensors Journal* 15, 3 (2015), 1538–1544.

[21] Chenshu Wu, Zheng Yang, Zimu Zhou, Kun Qian, Yunhao Liu, and Mingyan Liu. 2015. PhaseU: Real-time LOS identification with WiFi. In *Computer Communications (INFOCOM), 2015 IEEE Conference on*. IEEE, 2038–2046.

[22] Kaishun Wu, Jiang Xiao, Youwen Yi, Min Gao, and Lionel M Ni. 2012. Fila: Fine-grained indoor localization. In *INFOCOM, 2012 Proceedings IEEE*. IEEE, 2210–2218.

[23] Jiang Xiao, Kaishun Wu, Youwen Yi, and Lionel M Ni. 2012. FIFS: Fine-grained indoor fingerprinting system. In *Computer Communications and Networks (ICCCN), 2012 21st International Conference on*. IEEE, 1–7.

[24] Yaxiong Xie, Zhenjiang Li, and Mo Li. 2015. Precise Power Delay Profiling with Commodity WiFi. In *Proceedings of the 21st Annual International Conference on Mobile Computing and Networking*. ACM, 53–64.

[25] Zheng Yang, Zimu Zhou, and Yunhao Liu. 2013. From RSSI to CSI: Indoor localization via channel response. *ACM Computing Surveys (CSUR)* 46, 2 (2013), 25.

[26] Dian Zhang and Lionel M Ni. 2009. Dynamic clustering for tracking multiple transceiver-free objects. In *Pervasive Computing and Communications, 2009. PerCom 2009. IEEE International Conference on*. IEEE, 1–8.